DSC on ovalbumin-hematite "tempera" paints: the role of water and pigment on protein stability

Francesca Saitta[c], Marco Signorelli[c], Emilia Bramanti[b], Silvia Pizzimenti[a], Chiara Pelosi[a], Celia Duce[a,], Dimitrios Fessas[c,*], Ilaria Bonaduce[a], Maria Rosaria Tinè[a]*

[a]*Dipartimento di Chimica e Chimica Industriale, Università di Pisa,* Via Moruzzi 13, 56124 Pisa, Italy

[b]*National Research Council of Italy, C.N.R., Istituto di Chimica dei Composti OrganoMetallici-ICCOM-UOS Pisa, Area di Ricerca, Via G. Moruzzi 1, 56124 Pisa, Italy*

[c]*DeFENS, Università degli Studi di Milano, Via Celoria 2, 20133 Milano, Italy*

Corresponding Authors: Prof. Dimitrios Fessas, DeFENS, Università di Milano, Via Celoria 2, 20133 Milano, Italy, e-mail: dimitrios.fessas@unimi.it, tel. +390250319219; Prof. Celia Duce, Dipartimento di Chimica e Chimica Industriale, Università di Pisa, Via Moruzzi 13, 56124 Pisa, Italy, e-mail: celia.duce@unipi.it, tel. +39 0502219311

Abstract

The role of water and hematite (Fe_2O_3) on the stability of ovalbumin-based model paint layers was investigated by means of DSC and FTIR. The aim of this research is to improve our understanding on the stability of paint layers based on proteinaceous media, assessing the water content and the pigment presence effects. Pigments may play a fundamental role in determining the structure of proteins in paint layers, thus affecting the possible interactions among proteins and the external environment, including humidity. Previous studies revealed that hematite affects the secondary structure of OVA in paint layers, although no experimental evidence of hematite/OVA covalent bonds has been reported in the literature. In this paper we investigate the synergic effect of water and hematite on OVA structure and stability. DSC analyses coupled with FTIR measures on protein hydration revealed that below 30% of humidity the amount of water strongly influence the protein structure and stability: the less the water content, the higher the protein stability. Furthermore, our results suggest that a water phase separation occurs in the presence of hematite for which, in water-limiting condition, the hematite's hydration shell becomes almost negligible if compared to the bulk

water available for the protein hydration because of the high protein-water affinity. Accordingly, the protein phase humidity is higher than the sample's nominal value. Paints at the same overall humidity exhibit different protein hydration state following the pigment/binder ratio, and in turn different resistance to damages throughout aging.

Keywords: Ovalbumin, DSC, tempera paints, hematite, FT-IR.

1. Introduction

Paints layers are generally made up of one or more ~~(mineral)~~ pigments and a fluid binder, which enables the pigments to be dispersed and to adhere to the preparatory plaster layer if any or, sometimes, directly to the support (linen, wood, etc.). Historically, binding media were natural products, including plant gums, drying oils, waxes and animal protein-based materials such as egg, casein and animal glue [1].

Historical paint artworks may exhibit conservation issues due to degradation processes that may establish upon ageing, and that depend on several factors. Among them, a relevant role is played by the humidity conditions and/or exposure to moisture during certain conservation treatments [2–9]. Therefore, museums and galleries dedicate efforts into controlling relative humidity and temperature values at exposition sites, as well as in storage facilities, and optimal conditions are object of research [10,11].

Understanding the physicochemical modifications of the paint constituents upon ageing is crucial in order to propose a model for their chemical and physical stability, to set up reliable analytical protocols for their analysis and to plan reliable procedures for their preservation. In this context, the artificial ageing of several proteinaceous binders used in the "tempera" technique, including ovalbumin (OVA), and their interactions with different pigments have been studied in model paint layers [12–14]. Such studies indicated that certain inorganic pigments induce a decrease in the protein thermal stability and a protein network labilization. Furthermore, aging can induce aggregation, oxidation of some amino acid side chains and hydrolysis of the polypeptide chain in both pure proteins and pigmented paint layers [12–16].

Azurite ($Cu_3(CO_3)_2(OH)_2$) and red lead (Pb_3O_4) have been shown to affect the secondary structure of OVA in paint layers and data suggest that covalent bonds are formed among the metals and the protein. On the other hand, though hematite (Fe_2O_3) seems to affect the structure of OVA in paint layers as well, no experimental evidence of hematite/OVA covalent bonds have been found [13].

It is well known that the stability of globular proteins generally depends on the aqueous environment (pH, presence of co-solutes, amount of solvent, etc.), based on the possible specific and/or not specific interactions that may establish [17–21]. Specifically, it is well known that in condensed systems a general protein stabilization trend occurs, moving from high to low humidity levels [22]. In protein-based paints, such a trend may constitute a basis to which refer when investigating the nature and evolution of pigment-protein interactions which establish upon film formation and ageing.

In this work we investigate further model paint layers based on OVA and OVA-hematite, focusing on the effect of the water content. The study is carried out by means of Differential Scanning Calorimetry (DSC) and Fourier Transform Infrared Spectroscopy (FTIR) to determine the structure and thermal stability of the protein [23–27]. The aim is to get better insights into the nature of the interactions that establishes among OVA and hematite in a paint layer, how this relates to the paint layer water content, and to highlight how this interaction affects the structure and thermal stability of the protein.

2. Materials and methods

2.1. Model paint layers preparation

Model paints were based on OVA (51541, lyophilized powder, Bresciani srl, Italy) alone and in mixture with hematite (Fe_2O_3). Paint layers were prepared by dissolving the OVA powder in water and by adding, in case of pigmented model paints, hematite until paintable impastos were obtained [13]. The paints were then applied with a brush onto glass microscope slides and were left to dry at non-controlled room conditions (exposed to air and at natural indoor day-night light) for over a month in order to assure nonsignificant variations on the final humidity. The paint layers were prepared according to the following pigment/binder ratios: 0:100, 12:88, 23:77, 52:48.

2.2. Differential scanning calorimetry

A DSC 2920 (TA Instrument, USA) calorimeter with stainless steel sealed pans was used and runs from 20°C to 150°C at 2°C·min^{-1} were performed in order to assess OVA thermal stability. An empty pan was used as reference and calibration was carried out with indium as standard. Samples were prepared by scratching the paint layer from the glass slides by means of a scalpel. In order to analyse increasing values of water content, rehydration was reached by adding water within the pans. Supplementary samples were prepared with lyophilized OVA powder hydrated and suspended by directly adding water within the pans. The final water content for each sample was assessed after the DSC analysis, on the cold pans, by piercing the pans and desiccating them at 105°C.

Data were analyzed following procedures reported in previous studies [28,29]. In brief, the excess heat capacity $C_P^{exc}(T)$, *i.e.* the difference between the apparent heat capacity $C_P(T)$ of the sample and the heat capacity of the protein "native state", $C_{P,N}(T)$ / J·K^{-1}·g$^{-1}_{protein}$, was recorded across the scanned temperature range. First-cycle heating profiles were considered since all the

systems showed irreversibility due to post-denaturation aggregation phenomena. Such effects, which result in exothermic traces, were neglected in the figures for the sake of clarity since such a topic is beyond the scope of this paper. Three replicates were performed for each model paint layer.

2.3. Fourier transform infrared spectroscopy

OVA samples from the model paints were scraped from the glass supports and mixed with variable amounts of water in an agate mortar in order to reach various levels of humidity (7%, 24%, 34%, and 56% w/w). One mg of protein containing the various water percentages were mixed with 100 mg of ground KBr and the pellet was analysed in transmittance mode without further manipulations. Infrared spectra were recorded using a Perkin-Elmer Spectrum One FTIR Spectrophotometer, equipped with a universal attenuated total reflectance accessory (ATRU) and a TGS detector. For each sample, 128 interferograms were recorded in order to obtain a suitable signal/noise ratio, averaged and Fourier transformed to produce a spectrum with a nominal resolution of 4 cm^{-1}. Spectrum software (Perkin-Elmer) and a written-in-house LabVIEW program for peak deconvolution were employed to run and process the spectra, respectively. ~~The LabVIEW program for peak fitting is described elsewhere~~ [30,31]. Further details are reported in Supplementary Material.

3. Results and discussion

3.1. Stability of ovalbumin towards the water content

Although a paint layer in a painting contains one or more pigments, a pigment-free OVA model paint layer was studied as reference in order to understand the behaviour of the protein alone with respect to the water content in the first place. To this aim we investigated samples of rehydrated OVA starting both from the unpigmented model paint layer and lyophilized OVA (see materials and methods section).

The DSC thermograms of pigment-free OVA paint layers rehydrated with different water contents are reported in *Figure 1a*.

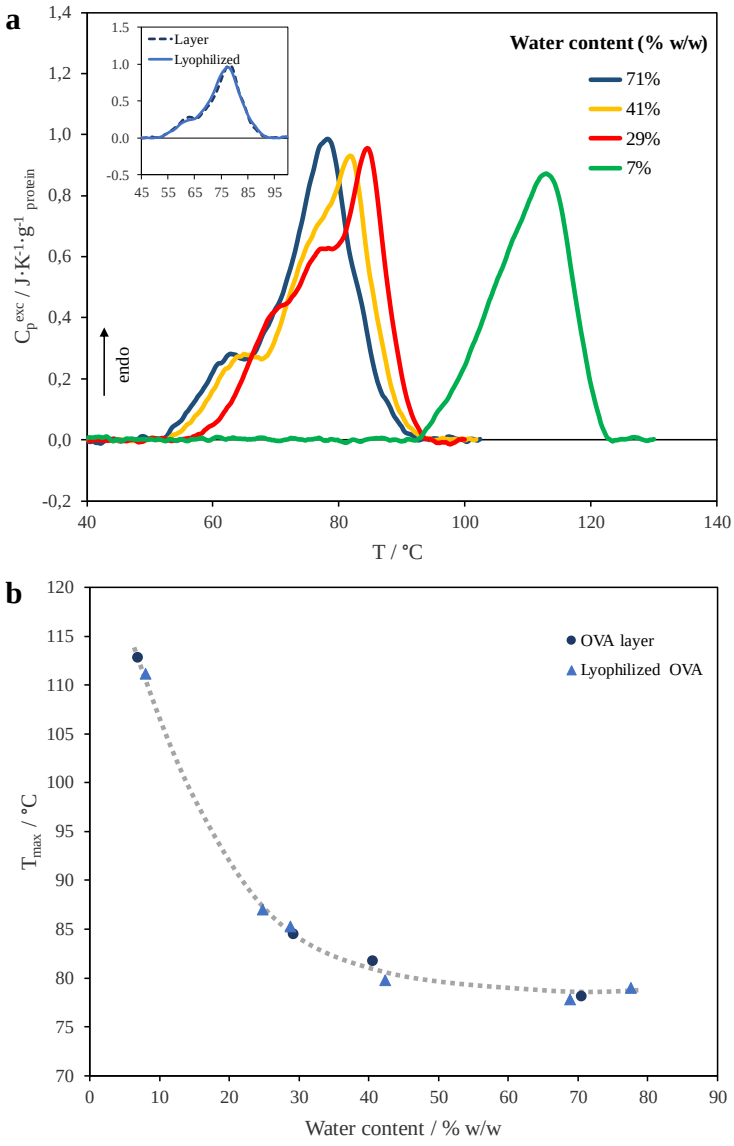

Figure 1*. a) DSC curves of unpigmented OVA model paint layer at different water content (% w/w). The inset shows the comparison between the DSC traces of unpigmented OVA model paint layer and lyophilized OVA-water suspension at 70% of water as an example. b) The maximum temperature (T_{max}) of the OVA DSC peak vs water content (% w/w) for both unpigmented OVA model paint layer and lyophilized powder suspensions. The points at the lowest water content correspond to the non-rehydrated OVA model paint layer and to the OVA powder used for the suspensions, i.e. both only containing their own intrinsic moisture.*

The DSC can be ascribed to the protein denaturation, where three superimposed peaks can be distinguished. Such profiles are in agreement with those typically obtained for chicken egg ovalbumin and reflect the distribution of the different ovalbumin conformers, namely the native ovalbumin (N-OVA, low-temperature shoulder), the intermediate form (I-OVA) and the stable ovalbumin (S-OVA, high-temperature peak), whose relative content depend on the kinetics of the N-to-S conversion and, in turn, on the OVA purification conditions [32–34].

A comparison of the thermograms obtained at high water content (about 70%) for both the rehydrated OVA model paint layer and lyophilized OVA-water suspension is also reported in the inset of *Figure 1a* as an example: thermograms are superimposable, suggesting that any possible mechanical stress deriving from the protein application onto glass surfaces to form paint layers and the subsequent water evaporation during drying and/or rehydration is not reflected in the protein thermal stability.

As far as the effects of the water content on the protein thermal stability are concerned (*Figure 1a*), we observe a progressive overall protein stabilization in terms of denaturation temperature range upshift when the amount of water decreases, whilst the enthalpic contribution due to OVA denaturation remains nearly unvaried ($\Delta_d H$ = 15 ± 2 J·g$^{-1}_{protein}$). After the denaturation temperature interval, aggregation phenomena were observed in most of the cases, whose onset depends on the water content, *i.e.* the higher the amount of water, the less proteins are prompt to aggregate [22]. These effects are neglected in the figure for the sake of clarity since such a topic is beyond the scope of this paper.

An overall picture of the influence of the water content on the protein thermal stability is shown in *Figure 1b*, where we report the denaturation peak maximum temperature, T_{max}, of the DSC thermograms versus the water content (% w/w). Indeed, the T_{max} is ascribable to the denaturation of the most stable form of ovalbumin (S-OVA) and is affected by only small shifts due to the superimposition of the denaturation of I-OVA form [32,33]. We observe a strong decreasing trend reaching a plateau at high water content, indicating the strong stabilizing effect of water-limiting condition. No differences were observed between the curves of the OVA model paint layer and the lyophilized OVA water suspension, as previously indicated (*Figure 1a*, inset).

Complementary information about the effects of different water contents on the structure of OVA were also obtained by means of FTIR analysis.

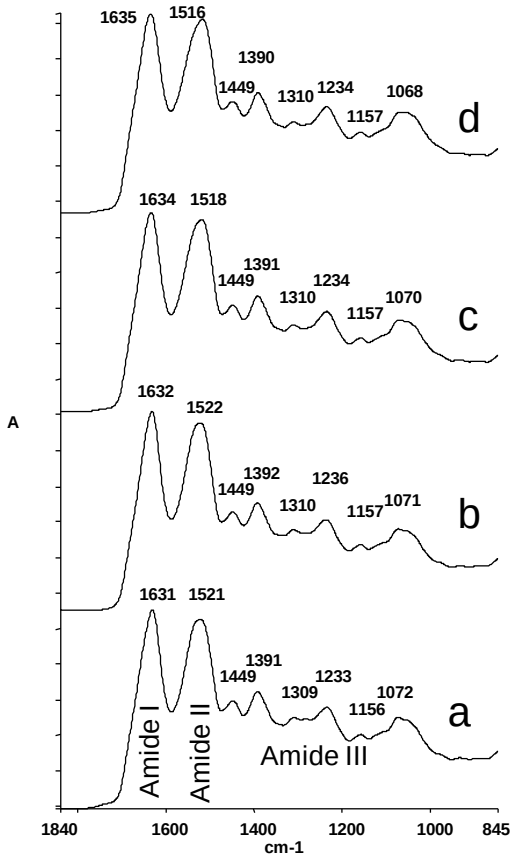

Figure 2. *ATIR-FTIR spectra in the region 1840-845 cm^{-1} of OVA at increasing water contents: (a) 7% w/w water; (b) 24% w/w water; (c) 34% w/w water; (d) 56% w/w water.*

Figure 2 shows the 1840-845 cm^{-1} region in the FTIR spectra of OVA model paint layers at increasing water contents. We observe the characteristic protein vibrational modes (Amide modes), which are sensitive to the protein conformation. In particular, Amide I (1700-1600 cm^{-1} region) is primarily due to the C=O stretching vibration, Amide II (1600-1480 cm^{-1} region) to the coupling of the N-H in-plane bending and C-N stretching modes, and Amide III (1350-1190 cm^{-1} region) to the C-N stretching coupled to the in-plane N-H bending mode [35].

The addition of water to OVA affects the region of the Amide I and Amide II bands, whose shifts are ascribable to conformational changes related to the polypeptide chain hydration: as the water content increases, the OVA Amide I band shifts from 1631 cm^{-1} to 1635 cm^{-1} and the Amide II shifts from 1521 cm^{-1} to 1516 cm^{-1}.

In order to gain further insights into the conformational changes due to hydration phenomena, we performed the spectral deconvolution of the Amide I band, which is the most reliable absorption widely employed for protein conformational analysis [12–15,30,31,36–39]. The conformational analysis of carbonyl stretching mode is therefore considered, and *Table 1* shows a summary of the results.

Table 1. *Summary of the secondary structure analysis of OVA at different content of water.*

OVA + 7% H_20 wavenumber/cm^{-1} (%)*	**OVA + 24% H_2O wavenumber/cm^{-1} (%)**	**OVA + 34% H_2O wavenumber/cm^{-1} (%)**	**OVA + 56% H_2O wavenumber/cm^{-1} (%)**	**Assignment**
1619 (32%)	1617 (27%)	1613 (15%)	1612 (3%)	β-Sheets (intermolecular)
1635 (25%)	1634 (31%)	1632 (39%)	1628 (39%)	β-Sheets (intramolecular)
1651 (4%)	1650 (6%)	1653 (23%)	1648 (25%)	Solvated α-Helix
1655 (19%)	1656 (20%)			Not solvated α-Helix
		1666 (5%)	1667 (22%)	extended Helix
1676 (19%)	1678 (16%)	1676 (19%)		β-Turns
			1690 (11%)	Antiparallel β-sheets

* The values in brackets, reported beside each wavenumber, represent the abundance of each protein secondary structure with respect to the total structures at the different water content conditions.

The band in the 1630–1640 cm^{-1} range and the weaker band around 1700–1690 cm^{-1} is assigned to antiparallel β-sheets [40]. Intermolecular β-sheets, typical of aggregate structures, present a band around 1610–1630 cm^{-1} [31,41–43].

Alpha-helix and random coil structures often give Amide I components overlapping in the range 1646 and 1657 cm^{-1}. Their position is affected by hydrogen bonds perturbed by the presence of bound water molecules that contribute to the distortion of the secondary structures of the polypetide chain. The component at 1651 and 1655 cm^{-1} of OVA has been ascribed to solvated (1651 cm^{-1}) and buried/not-solvated α-helices (1655 cm^{-1}) [44,45]. Absorptions at 1666–1667 cm^{-1} are associated with an extended helix or 3_{10}-helix structure [46].

Data reported in *Table 1* show that hydration promotes the decrease of intermolecular β-sheets and a corresponding increase of intramolecular β-sheets, as well as the increase of solvated α-helix content (*Figure 3A*).

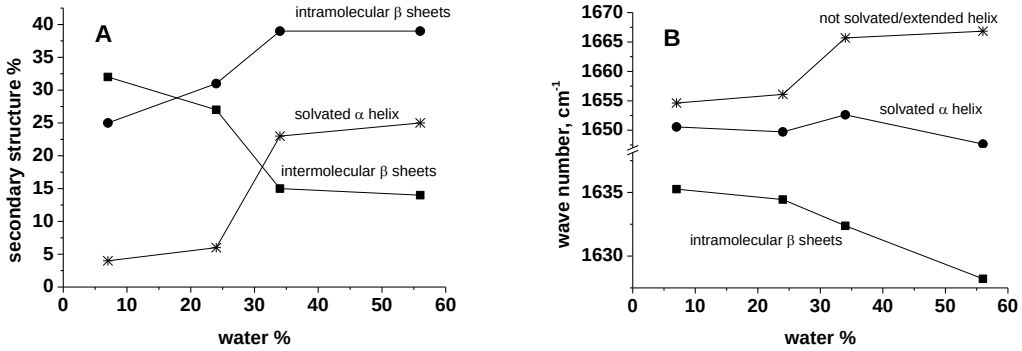

Figure 3. *β-sheet and α-helix relative contents (a) and shifts of bands ascribable to intramolecular β-sheets and α-helix structures as a function of water relative content (b).*

The hydration of the OVA structure is well evidenced also by the downshift of intramolecular β-sheets [35] (*Figure 3B*). The solvated α-helix component does not present a significant shift.

It is interesting to observe that the protein is completely hydrated for water content >30% w/w as shown by the disappearance of not solvated helix (1655 cm^{-1}) and the appearance of a new component at 1666 cm^{-1} assigned to extended helix.

This observation is supported by the DSC data (*Figure 1b*): indeed, only modest variations on the protein stability can be observed for water content >30% w/w, whereas small changes in the water content severely affect both the protein thermal stability (*Figure 1b*) and secondary structure (*Figure 3*) when the water content decreases below 30%.

3.2. Hematite influence on ovalbumin stability in paint layers

In this study three hematite-containing paint layers with different pigment/binder ratios (12:88, 23:77 and 52:48) were investigated. *Figure 4* shows the DSC profiles of samples of the hematite:OVA 12:88 model paint layer at different values of relative water content (% w/w) as an example.

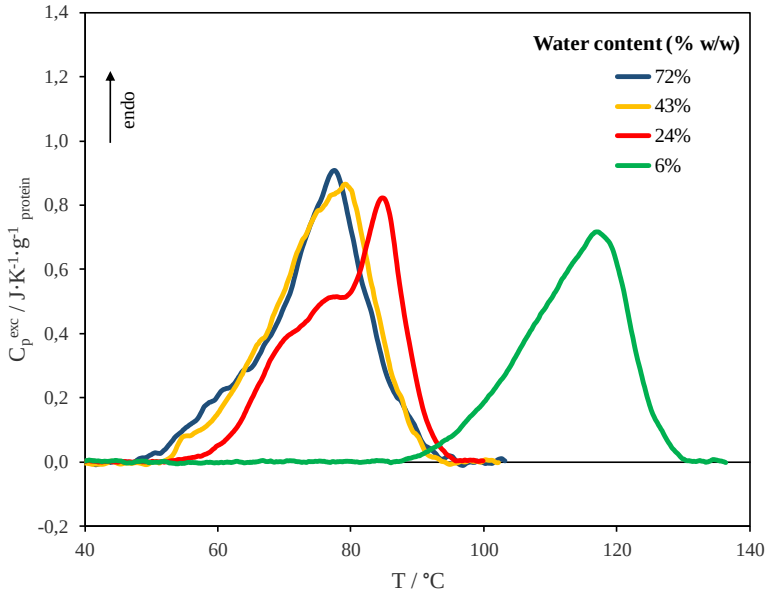

Figure 4. *DSC curves of samples from the 12:88 hematite:OVA model paint layers at different relative water content (% w/w). The profile at the lowest relative water content corresponds to the non-rehydrated sample, i.e. only containing its own intrinsic moisture.*

A similar behaviour to the unpigmented model paint layer (*Figure 1a*) is observed: the lower the water content, the higher the overall protein stabilization (upshift of the denaturation temperature range). The overall enthalpies are of the same order of magnitude (about 15 $J \cdot g^{-1}_{protein}$) as for the unpigmented model paint layer. However, the enthalpies for pigmented paint layers were affected by a larger variability, given the inhomogeneity of the protein relative content in the pigmented paint layer, and the enthalpy average value obtained for pigment-free layers was used to normalize the thermograms in *Figure 4* only for the sake of visibility and comparison. For this reason, we only focus on the intensive property, *i.e.* the denaturation peak maximum temperature T_{max}, as a parameter to evaluate the protein stability in order to perform reliable comparisons among different samples.

In *Figure 5a*, we report the T_{max} obtained from the DSC thermograms for the three pigmented paint layers versus the relative water content. Although a similar general trend is observed if compared to *Figure 1b*, *i.e.* the T_{max} decreases as the water content increases, the trend is not as regular as that observed for the unpigmented model paint layers, and differences and deviations from this reference pattern (dotted grey curve) become larger as the pigment/protein ratio increases.

However, if we plot the T_{max} versus the % w/w relative water content calculated as water/(protein+water) ratio, excluding the hematite weight, data become regular and perfectly fit the same trend observed with the unpigmented model paint layer, as shown in *Figure 5b*.

This scenario suggests the presence of a water phase separation, according to which the high protein-water affinity dominates making the hematite's hydration shell almost negligible if compared to the bulk water available for the protein hydration [22].

Accordingly, we could ascribe the destabilization and structure modification of OVA, when in the presence of hematite, mostly to a water redistribution in the pigmented paint layer. This effect is more evident at low humidity ranges and at high pigment percentages, and justifies the effects observed in a previous work [13]. In other words, combining the previous results with the present ones, if we consider paint layers with increasing hematite/OVA ratio at the same sample water content, we may state that richer paints in hematite are characterized by more hydrated protein, and are hence more labile and subjected to damages throughout aging.

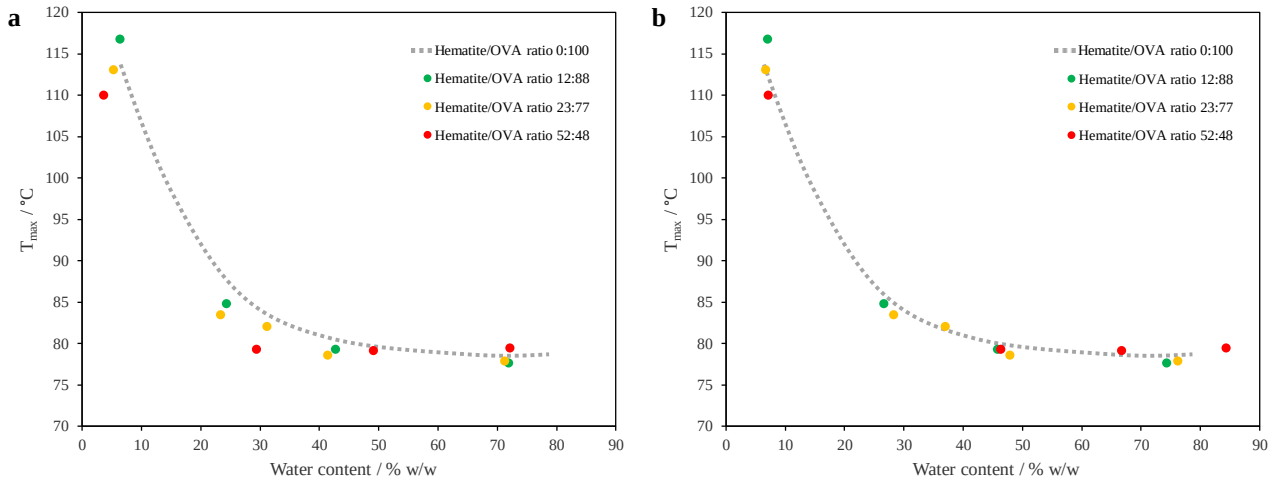

Figure 5*. a) The maximum temperature (T_{max}) of the OVA DSC peak vs sample water content (% w/w) for hematite:OVA paint layer samples with pigment:binder ratios of 0:100 (dotted grey line), 12:88, 23:77, 52:48; b) The maximum temperature (T_{max}) of the OVA unfolding peak vs "protein" water content (% $w_{water}/w_{protein+water}$) for the same samples from panel a. The points at the lowest water contents for the respective layers correspond to the non-rehydrated samples, i.e. only containing their own intrinsic moisture.*

4. Conclusions

In this work we investigated the effect of different levels of water on the stability of OVA/hematite paint layers by evaluating the denaturation process of OVA through DSC.

The preliminary comparison between the DSC profiles of both lyophilized OVA suspensions and OVA layers assessed the absence of any injury on OVA native structure due to a mechanical stress linked to protein application on glass surfaces as well as to the protein layer drying.

Calorimetric data on the protein stability, coupled with FTIR information on protein secondary structure and chain hydration, revealed that the water effects on the protein structure become relevant when the relative water content is below 30%, and that a strong stabilization occurs as the water content decreases. Indeed, under water-limiting conditions as is the case of paint layers, small changes in the water content of the paint layer may produce significant effects on protein stability and structure.

The DSC analysis of protein stability under different humidity conditions in hematite/OVA model paint layers strongly suggests that a water phase separation occurs within the paint, and the hematite's hydration shell seems almost negligible with respect to the bulk water available for the protein hydration. Accordingly, the protein phase water content is higher than the sample's nominal value, resulting in a destabilization of OVA in the paint layer. For this reason, this work suggests that water phase separations must be always assessed for protein-pigment "tempera" paints since protein stability strongly depends on protein phase humidity.

Nevertheless, we underline that the present work is focused on the folded-state OVA stability in paints, discriminating from the effects of hematite on aggregates and/or networks formed after protein denaturation, which may occur during a long-time span conservation [13].

The data strongly indicate how controlling the environmental parameters at exposure and conservation sites of museum objects may play a fundamental role in ensuring the stability of protein-based paint layers, avoiding issues related to changes in the protein structure upon changes in humidity.

5. Acknowledgements

Financial support of "Advanced analytical pyrolysis to study polymers in renewable energy, environment, cultural heritage, Progetto di Ricerca di Ateneo dell'Università di Pisa, PRA_2018_26" is acknowledged.

6. References

[1] R. Mayer, The artist's handbook of materials and techniques, 1991.

[2] E. Hagan, E. Quasney, M. Mecklenburg, A Parametric Analysis of Relative Humidity Effects on Traditional Panel Paintings, MRS Proc. 852 (2004) OO2.8. doi:DOI: 10.1557/PROC-852-OO2.8.

[3] J.D. Erlebacher, E. Brown, M.F. Mecklenburg, C.S. Tumosa, The Effects of Temperature and Relative Humidity on the Mechanical Properties of Modern Painting Materials, MRS Proc. 267 (1992) 359. doi:DOI: 10.1557/PROC-267-359.

[4] M.F. Mecklenburg, C.S. Tumosa, Mechanical behavior of paintings subjected to changes in temperature and relative humidity, 1991.

[5] M. Doutre, A. Murray, L. Fuster-López, Effects of Humidity on Gessoes for Easel Paintings, MRS Proc. 1656 (2017) 167–171. doi:DOI: 10.1557/opl.2014.828.

[6] M.F. Mecklenburg, L. Fuster Lopez, Failure Mechanisms in Canvas Supported Pain-tings: Approaches for Developing Consolidation Protocols, in: Care Paint. Surfaces. Mater. Methods Consol. Sci. Methods to Eval. Their Eff. Proc. Conf. Milan, Novemb. 10-11, 2006 (Third Int. Conf. Colour Conserv. Mater., 2006: pp. 49–58.

[7] M.C. Area, H. Cheradame, Paper aging and degradation: recent findings and research methods, BioResources. (2011). doi:10.15376/biores.6.4.5307-5337.

[8] F. Modugno, F. Di Gianvincenzo, I. Degano, I.D. van der Werf, I. Bonaduce, K.J. van den Berg, On the influence of relative humidity on the oxidation and hydrolysis of fresh and aged oil paints, Sci. Rep. 9 (2019) 5533. doi:10.1038/s41598-019-41893-9.

[9] D. Saunders, J. Kirby, The effect of relative humidity on artists' pigments, Natl. Gall. Tech. Bull. 25 (2004) 62–72.

[10] D. Erhardt, M. Mecklenburg, Relative humidity re-examined, Stud. Conserv. 39 (1994) 32–38. doi:10.1179/sic.1994.39.Supplement-2.32.

[11] S. Jakiela, R. Kozlowski, Allowable thresholds in dynamic changes of microclimate for wooden cultural objects: monitoring in situ and modelling, in: ICOM Comm. Conserv. 14th Trienn. Meet. Hague, 12-16 Sept. 2005 Prepr., James & James, London, 2005: pp. 582–589.

[12] C. Duce, L. Ghezzi, M. Onor, I. Bonaduce, M.P. Colombini, M.R. Tine', E. Bramanti, Physico-chemical characterization of protein-pigment interactions in tempera paint reconstructions: Casein/cinnabar and albumin/cinnabar, Anal. Bioanal. Chem. 402 (2012) 2183–2193. doi:10.1007/s00216-011-5684-x.

[13] C. Duce, E. Bramanti, L. Ghezzi, L. Bernazzani, I. Bonaduce, M.P. Colombini, A. Spepi, S. Biagi, M.R. Tinè, Interactions between inorganic pigments and proteinaceous binders in reference paint reconstructions, Dalt. Trans. 42 (2013) 5975–5984. doi:10.1039/C2DT32203J.

[14] L. Ghezzi, C. Duce, L. Bernazzani, E. Bramanti, M.P. Colombini, M.R. Tiné, I. Bonaduce,

Interactions between inorganic pigments and rabbit skin glue in reference paint reconstructions, J. Therm. Anal. Calorim. 122 (2015) 315–322. doi:10.1007/s10973-015-4759-x.

[15] S. Orsini, E. Bramanti, I. Bonaduce, Analytical pyrolysis to gain insights into the protein structure. The case of ovalbumin, J. Anal. Appl. Pyrolysis. 133 (2018) 59–67. doi:10.1016/j.jaap.2018.04.020.

[16] S. Orsini, F. Parlanti, I. Bonaduce, Analytical pyrolysis of proteins in samples from artistic and archaeological objects, J. Anal. Appl. Pyrolysis. 124 (2017). doi:10.1016/j.jaap.2016.12.017.

[17] C. Pelosi, F. Saitta, F.R. Wurm, D. Fessas, M.R. Tinè, C. Duce, Thermodynamic stability of myoglobin-poly(ethylene glycol) bioconjugates: A calorimetric study, Thermochim. Acta. 671 (2019) 26–31. doi:10.1016/j.tca.2018.11.001.

[18] C. Pelosi, C. Duce, D. Russo, M.R. Tiné, F.R. Wurm, PPEylation of proteins: Synthesis, activity, and stability of myoglobin-polyphosphoester conjugates, Eur. Polym. J. 108 (2018) 357–363. doi:10.1016/j.eurpolymj.2018.09.019.

[19] M. D'Onofrio, L. Ragona, D. Fessas, M. Signorelli, R. Ugolini, M. Pedò, M. Assfalg, H. Molinari, NMR unfolding studies on a liver bile acid binding protein reveal a global two-state unfolding and localized singular behaviors, Arch. Biochem. Biophys. 481 (2009) 21–29. doi:10.1016/j.abb.2008.10.017.

[20] M. Guariento, M. Assfalg, S. Zanzoni, D. Fessas, R. Longhi, H. Molinari, Chicken ileal bile-acid-binding protein: a promising target of investigation to understand binding co-operativity across the protein family, Biochem. J. 425 (2010) 413–424. doi:10.1042/BJ20091209.

[21] L. Caldinelli, S. Iametti, A. Barbiroli, D. Fessas, F. Bonomi, L. Piubelli, G. Molla, L. Pollegioni, Relevance of the flavin binding to the stability and folding of engineered cholesterol oxidase containing noncovalently bound FAD, Protein Sci. 17 (2008) 409–419. doi:10.1110/ps.073137708.

[22] D. Fessas, M. Signorelli, A. Pagani, M. Mariotti, S. Iametti, A. Schiraldi, Guidelines for buckwheat enriched bread, J. Therm. Anal. Calorim. 91 (2008) 9–16. doi:10.1007/s10973-007-8594-6.

[23] J.W. Donovan, C.J. Mapes, J.G. Davis, J.A. Garibaldi, A differential scanning calorimetric study of the stability of egg white to heat denaturation, J. Sci. Food Agric. 26 (1975) 73–83. doi:10.1002/jsfa.2740260109.

[24] M. Rossi, A. Schiraldi, Thermal denaturation and aggregation of egg proteins, Thermochim. Acta. 199 (1992) 115–123. doi:10.1016/0040-6031(92)80255-U.

[25] M. Ferreira, C. Hofer, A. Raemy, A calorimetric study of egg white proteins, J. Therm. Anal. 48 (1997) 683–690. doi:10.1007/BF01979514.

[26] N. Matsudomi, H. Takahashi, T. Miyata, Some structural properties of ovalbumin heated at 80°C in the dry state, Food Res. Int. 34 (2001) 229–235. doi:10.1016/S0963-9969(00)00157-5.

[27] D. Sharma, Non-isothermal unfolding/denaturing kinetics of egg white protein, J. Therm. Anal. Calorim. 109 (2012) 1139–1143. doi:10.1007/s10973-012-2225-6.

[28] G. Barone, P. Del Vecchio, D. Fessas, C. Giancola, G. Graziano, Theseus: A new software package for the handling and analysis of thermal denaturation data of biological macromolecules, J. Therm. Anal. 38 (1992) 2779–2790. doi:10.1007/BF01979752.

[29] A. Ausili, A. Pennacchio, M. Staiano, J.D. Dattelbaum, D. Fessas, A. Schiraldi, S. D'Auria, Amino acid transport in thermophiles: Characterization of an arginine-binding protein from Thermotoga maritima. 3. Conformational dynamics and stability, J. Photochem. Photobiol. B Biol. 118 (2013) 66–73. doi:https://doi.org/10.1016/j.jphotobiol.2012.11.004.

[30] E. Bramanti, M. Bramanti, P. Stiavetti, E. Benedetti, A frequency deconvolution procedure using a conjugate gradient minimization method with suitable constraints, J. Chemom. 8 (1994) 409–421. doi:10.1002/cem.1180080606.

[31] E. Bramanti, E. Benedetti, A. Sagripanti, F. Papineschi, E. Benedetti, Determination of secondary structure of normal fibrin from human peripheral blood, Biopolymers. 41 (1997) 545–553. doi:10.1002/(SICI)1097-0282(19970415)41:5<545::AID-BIP6>3.0.CO;2-M.

[32] J. de Groot, H.H.J. de Jongh, The presence of heat-stable conformers of ovalbumin affects properties of thermally formed aggregates, Protein Eng. Des. Sel. 16 (2003) 1035–1040. doi:10.1093/protein/gzg123.

[33] H. Hatta, M. Nomura, N. Takahashi, M. Hirose, Thermostabilization of Ovalbumin in a Developing Egg by an Alkalinity-regulated, Two-step Process, Biosci. Biotechnol. Biochem. 65 (2001) 2021–2027. doi:10.1271/bbb.65.2021.

[34] J.W. Donovan, C.J. Mapes, A differential scanning calorimetric study of conversion of ovalbumin to S- ovalbumin in eggs, J. Sci. Food Agric. 27 (1976) 197–204. doi:10.1002/jsfa.2740270220.

[35] A. Barth, Infrared spectroscopy of proteins, Biochim. Biophys. Acta - Bioenerg. 1767 (2007) 1073–1101. doi:10.1016/j.bbabio.2007.06.004.

[36] E. Bramanti, E. Benedetti, Determination of the secondary structure of isomeric forms of human serum albumin by a particular frequency deconvolution procedure applied to Fourier transform IR analysis, Biopolymers. 38 (1996).

[37] C. Duce, E. Bramanti, L. Ghezzi, L. Bernazzani, I. Bonaduce, M.P. Colombini, A. Spepi, S. Biagi, M.R. Tine, Interactions between inorganic pigments and proteinaceous binders in reference paint reconstructions, Dalt. Trans. 42 (2013). doi:10.1039/c2dt32203j.

[38] E. Bramanti, E. Benedetti, C. Nicolini, T. Berzina, V. Erokhin, A. D'Alessio, E. Benedetti, Qualitative and quantitative analysis of the secondary structure of cytochrome C Langmuir-Blodgett films, Biopolymers. 42 (1997). doi:10.1002/(SICI)1097-0282(199708)42:2<227::AID-BIP11>3.0.CO;2-I.

[39] S. Orsini, E. Bramanti, I. Bonaduce, Analytical pyrolysis to gain insights into the protein structure. The case of ovalbumin, J. Anal. Appl. Pyrolysis. (2018). doi:10.1016/j.jaap.2018.04.020.

[40] Y.N. Chirgadze, O. V. Fedorov, N.P. Trushina, Estimation of amino acid residue side-chain absorption in the infrared spectra of protein solutions in heavy water, Biopolymers. 14 (1975) 679–694. doi:10.1002/bip.1975.360140402.

[41] I.H.M. van Stokkum, H. Linsdell, J.M. Hadden, P.I. Haris, D. Chapman, M. Bloemendal, Temperature-Induced Changes in Protein Structures Studied by Fourier Transform Infrared Spectroscopy and Global Analysis, Biochemistry. 34 (1995) 10508–10518. doi:10.1021/bi00033a024.

[42] T. Heimburg, J. Schuenemann, K. Weber, N. Geisler, Specific recognition of coiled coils by infrared spectroscopy: Analysis of the three structural domains of type III intermediate filament proteins, Biochemistry. 35 (1996) 1375–1382. doi:10.1021/bi9515883.

[43] A. Muga, H.H. Mantsch, W.K. Surewicz, Membrane binding induces destabilization of cytochrome c structure, Biochemistry. 30 (1991) 7219–7224. doi:10.1021/bi00243a025.

[44] H. Torii, M. Tasumi, Model calculations on the amide-I infrared bands of globular proteins, J. Chem. Phys. 96 (1992) 3379–3387. doi:10.1063/1.461939.

[45] N.A. Nevskaya, Y.N. Chirgadze, Infrared spectra and resonance interactions of amide-I and II vibrations of α-helix, Biopolymers. 15 (1976) 637–648. doi:10.1002/bip.1976.360150404.

[46] D.F. Kennedy, M. Crisma, C. Toniolo, D. Chapman, Studies of peptides forming 310- and α-helixes and β-bend ribbon structures in organic solution and in model biomembranes by Fourier transform infrared spectroscopy, Biochemistry. 30 (1991) 6541–6548. doi:10.1021/bi00240a026.